Icarus 221 (2012) 806–815

Contents lists available at SciVerse ScienceDirect

Icarus

journal homepage: www.elsevier.com/locate/icarus

On the formation of the martian moons from a circum-martian accretion disk

Pascal Rosenblatt [a,*], Sébastien Charnoz [b,c]

[a] Royal Observatory of Belgium (ROB), Av. Circulaire 3, B-1180 Uccle, Belgium
[b] Laboratoire AIM, UMR 7158, Université Paris Diderot/CEA IRFU/CNRS, Centre de l'Orme les Merisiers, 91191 Gif sur Yvette Cedex, France
[c] Institut Universitaire de France, 103 Boulevard Saint Michel, 75005 Paris, France

ARTICLE INFO

Article history:
Received 24 March 2012
Revised 8 September 2012
Accepted 11 September 2012
Available online 27 September 2012

Keywords:
Mars, Satellites
Satellites, formation
Accretion

ABSTRACT

We reconsider two scenarios for the formation of Phobos and Deimos from a circum-martian accretion disk of debris: the strong tide regime for which accretion occurs close to the planet at the Roche limit and the weak tide regime for which accretion occurs farther from the planet. We assume a disk with an initial mass of 10^{18} kg (Craddock, R.A. [2011]. Icarus 211, 1150–1161). In the strong tide regime, the disk loses its material by viscous spreading inward to and outward from the planet. When outward moving material crosses the Roche limit, small-sized moonlets are accreted from gravitational instabilities with a shape and density similar to Phobos and Deimos. Due to the gravitational torque exerted by the disk, the moonlets migrate away from the planet, though they cannot reach the synchronous orbit (lying at 6 Mars' radii). After the disk has lost most of its mass they rapidly fall back onto Mars due to the tidal decay of their orbits. Although, the total mass of moonlets is comparable to the mass of Phobos, their survival time does not exceed 200 Ma, which is incompatible with the formation of Phobos and Deimos early in Mars' history. In the weak tide regime, moonlets can accrete near the synchronous orbit with the mass of Deimos in a disk of up to 10^{18} kg (similarly to planetary embryos formation in the protoplanetary disk). A Phobos-mass embryo can also be formed in the same disk but closer to Mars (at 3–4 Mars' radii) so that it rapidly falls back onto Mars by tidal decay of its orbit. However, several embryos may accrete together in the disk (similarly to the final stage of terrestrial planet formation), and Phobos and Deimos may be the last two remnants of those bodies formed near the synchronous distance to Mars. Further investigations are still needed to understand such accretion mechanism within a circum-martian disk primarily extending below the synchronous orbit.

1. Introduction

The origin of the martian moons, Phobos and Deimos, is still an open issue in spite of numerous spacecraft missions sent to the martian system. It has been proposed that both moons are asteroids captured by Mars' gravitational attraction (e.g. Burns, 1992) or that they formed *in situ* from a disk of debris in Mars' orbit (e.g. Peale, 2007). The capture scenario is mainly based on similarities between the physical characteristics of the surface of the moons and those of some small-sized low-albedo carbonaceous asteroids. Although this scenario has prevailed in the literature for a long time, it has some weaknesses, in particular, the difficulty to account for the current near-circular and near-equatorial orbits of both moons, and the ambiguity in the identification of their true composition from the remote-sensing observations of their surfaces (e.g. Rosenblatt, 2011).

On the other hand, the martian moon orbits are consistent with the expected orbits of objects accreted around Mars (Safronov et al., 1986) that led several authors to propose some scenarios where both moons were formed from material orbiting Mars (i.e. *in situ* formation scenarios). Some of these scenarios are not inconsistent with a composition of Phobos and Deimos different from the martian composition, since they involve the entering of an object from the outer part of the Solar System (so, possibly of carbonaceous composition) into Mars orbit (e.g. Singer et al., 2007; Craddock, 2011). Unlike the capture scenario, the *in situ* formation scenarios have not been studied in detail so far, thus making them somewhat *ad hoc* scenarios (e.g. Rosenblatt, 2011).

Recent observations of Phobos made by the Mars Express (MEX) spacecraft have raised a renewed interest in these *in situ* scenarios. In particular, the determination of the bulk density of Phobos has been significantly improved, and has been interpreted as evidence supporting a gravitational aggregate structure for the interior of Phobos, which may result from its formation by accretion of debris in Mars' orbit (Andert et al., 2010; Rosenblatt, 2011). Moreover, new remote-sensing observations of Phobos' surface suggest that its surface is composed of material similar to the material of Mars' surface (Giuranna et al., 2011). Although these recent observations cannot disprove the capture scenario, they have been interpreted

* Corresponding author. Fax: +32 2 3749822.
E-mail addresses: rosenb@oma.be, Pascal.Rosenblatt@oma.be (P. Rosenblatt).

0019-1035/$ - see front matter © 2012 Elsevier Inc. All rights reserved.
http://dx.doi.org/10.1016/j.icarus.2012.09.009

as evidence supporting *in situ* formation for this moon (Rosenblatt, 2011).

One of the *in situ* scenarios proposes that Phobos and Deimos were formed early in the martian history from gravitational instabilities within a circum-martian accretion disk, resulting from a giant collision between Mars and a large object (Craddock, 2011, see also Section 2). Recently, a physical model of accretion from gravitational instabilities has been proposed to account for the formation of the small irregular-shaped moons of Saturn from the material of its main rings (Charnoz et al., 2010). However, no such modeling has been done so far to study the formation of the martian moons, thus leaving unexplored the expected physical properties of the objects accreted in Mars' orbit (i.e. shape, mass, density) with regard to those of Phobos and Deimos as well as the required compatibility with the current orbital configuration of the martian system (Rosenblatt, 2011).

In this study, we rely on current theories of accretion to establish a physical framework for the formation of Phobos and Deimos in a circum-martian accretion disk. It is shown that two main regimes of accretion can occur: the strong tide regime for which accretion occurs close to the planet at the Roche limit and the weak tide regime for which accretion occurs farther from the planet where tides do not play a significant role in the accretion process. The former regime has been shown to work for the formation of the Moon of the Earth (e.g. Canup, 2004), and more recently for the formation of Saturn's icy moons (Charnoz et al., 2010, 2011), while the latter regime has been shown to work for the formation of the big satellites of Jupiter and Saturn, and is inspired from numerous works about the formation of planetary embryos (e.g. Lissauer, 1987).

The *in situ* formation scenario proposed by Craddock (2011) is summarized in Section 2, and will be used as a basis for exploring the physics of accretion within a circum-martian disk. Section 3 and 4 describe the general properties of accretion in the strong tide and the weak tide regimes, respectively, and explore their consequences for the formation of the martian moons. The results obtained in Section 3 and 4 are discussed in Section 5.

2. Formation of a martian accretion disk of debris from a giant impact

One of the *in situ* formation scenarios proposes that Phobos and Deimos were formed early in Mars' history from a giant impact between Mars and a large body (1800 km in diameter, Craddock, 2011). In this scenario, the impact would have given to Mars its current spin rate, and the debris inserted into orbit would have formed a disk around Mars, which could extend slightly beyond the current Mars' synchronous orbit (lying at 6 Mars' radii). Gravitational instabilities would have then occurred within this disk (at distances beyond the Roche limit of Mars) from which small-sized objects or moonlets would have been accreted. Once the disk dissipated, most of these moonlets would have fallen back to Mars due to the tidal decay of their orbits. These fallen moonlets would have fed the elongated crater population at the martian surface (e.g. Schultz and Lutz-Garihan, 1982; Buchenberger et al., 2011), and Phobos and Deimos would be the last two remnants of this population of moonlets.

In this scenario, the orbits of the moonlets are expected to be near-equatorial and near-circular, and a carbonaceous composition for Phobos and Deimos could be accounted for, if the impactor was of carbonaceous composition. Indeed, the debris blasted into Mars' orbit from such a collision could come mainly from the impactor, depending on the velocity and the angle of the collision, as shown in the Earth–Moon case (e.g. Cameron, 1986).

However, this scenario has not been studied in detail, yet it relies on several assumptions. For instance, the mass of the impactor has been computed by assuming that the current spin rate of Mars has been acquired from one single collision, yielding an impactor mass of 9.61×10^{21} kg (Craddock, 2011). In addition, the amount of material ejected into orbit from this collision has been estimated from the population of elongated craters on Mars, resulting in a mass of the accretion disk of about 10^{18}–10^{19} kg (or 0.01–0.4% of the computed mass of the impactor). However, as emphasized in Craddock (2011), this estimate is uncertain since crater scaling laws can provide only a rough estimate of the amount of ejected material by impact processes. Moreover, a significant fraction of this elongated crater population may also result from asteroid impactors and not from the orbital decay of former moonlets (Bottke et al., 2000). The scenario also assumes that half of the disk material has been used to form moonlets, and that gravitational instabilities occurred within the whole disk.

In spite of these limitations, this scenario provides the most precise framework so far for physical studies of the formation of Phobos and Deimos in a circum-martian accretion disk. It implies physical processes (i.e. gravitational instabilities) similar to the ones occurring in a strong tide regime of accretion such as in the model recently proposed to explain the formation of the small moons of Saturn from its rings (Charnoz et al., 2010, 2011). That model has shown that when Saturn's rings spread beyond the Roche limit, they become gravitationally unstable and give birth to small-sized aggregates. Through subsequent mutual accretion these aggregates grow, then they recede away from the planet due to their tidal interaction with the planet and the rings. This model accounts for the mass-distance distribution of the small moons of Saturn (i.e. the more massive, the more distant to the rings). In the next section, we propose to apply this model to the evolution of a martian gravitationally unstable accretion disk and the formation of aggregates from it by adapting the hybrid code developed for Saturn's moons to Mars.

3. The strong tide regime of accretion

3.1. Basic physics: shape and density of accreted objects

After the giant impact on the planet, the ejected debris form a cloud of particles around Mars. The collisions between the particles induce a net energy loss while the angular momentum is conserved. As a result, the cloud flattens into a disk in a time comparable to the collisional timescale. This kind of flattening mechanism has been first numerically investigated in Brahic and Henon (1977), and clearly appears in N-body simulations of the Earth's Moon formation (e.g. Kokubo and Ida, 2000). Due to its own viscosity, the disk spreads outward from the planet, at an increasing rate as the disk is gravitationally unstable (see Salmon et al., 2010). When the disk material crosses the Roche limit of the planet, the gravitational instabilities set-in and aggregates are formed in a time comparable to the orbital period of the disk particles (Kokubo and Ida, 2000; Karjalainen and Salo, 2004; Karjalainen, 2007; Charnoz et al., 2010, 2011). Then, these aggregates collide, accreting material inside their local sphere of gravitational influence (the Hill sphere). As the accretion occurs close to the planet, it is controlled by Mars' tides and it stops when the Hill sphere of the accreting body is filled up entirely by disk material (e.g. Canup and Esposito, 1997). As a consequence, the accreted body (or moonlet) has a shape and a density given by those of the Hill sphere (Karjalainen, 2007; Porco et al., 2007). Due to the proximity to the planet (large tidal forces), the shape of this Hill sphere is a triaxial ellipsoid with a 3:2:2 axes ratio (the longest axis being directed toward the planet, Porco et al., 2007). The Hill sphere density, also called the critical density ρ_{crit}, depends on the mass of the planet M_p and on the distance a of the accreted moonlet to the planet center of mass, as follows (Porco et al., 2007):

$$\rho_{crit} = \frac{M_P}{1.59a^3} \tag{1}$$

The critical density rapidly decreases as the distance to the planet is increasing (Fig. 1). Depending on the density of the accreted material, the accreted object is expected to have some amount of porosity in its interior in order to fit the critical density of the Hill sphere. Therefore, a gravitational aggregate structure for the interior of this accreted object is expected, if the material density is significantly larger than the critical density.

The bulk properties of the martian moons (shape and density) are similar to those of moonlets accreted in the strong tide regime. Indeed, the shape of the martian moons can be approximated by a triaxial ellipsoid with aspect ratios corresponding roughly to the expected 3:2:2 ratio of the Hill sphere of the objects formed near the Roche limit (see Table 1). In addition, the density of the martian moons corresponds to the Hill sphere critical density for a distance to Mars of about 2.5 Mars' radii (Fig. 1), which nearly corresponds to the Roche limit of Mars. Therefore, both shape and density of Phobos and Deimos are compatible with those expected for moonlets accreted near the Roche limit of Mars. Moreover, such an origin would explain why the martian moons have a density lower than the density of possible material analogs (Rosenblatt, 2011). However, Phobos and especially Deimos are currently orbiting at larger distances to Mars than the Roche limit (at 2.5 Mars' radii). Here we investigate the orbital evolution of the moonlets accreted at the Roche limit over long time-scales (a few billions years) as well as the number that can be produced and the mass they can have. To this goal, we have adapted a hybrid model initially developed for the formation of Saturn's moons from the rings of the planet (Charnoz et al., 2010, 2011) to Mars.

3.2. Evolution of a gravitationally unstable accretion disk around Mars

3.2.1. Modeled physics

The long timescale evolution of a gravitationally unstable disk around Mars and of the associated system of moonlets is governed by the evolution of the disk itself and of its gravitational interaction with the moonlets as well as by the tidal interaction between the planet and the moonlets. In order to take these two interactions into account, we use the hybrid model described in Charnoz et al. (2010, 2011) and in Salmon et al. (2010) for the rings of Saturn. This model consists of coupling in a self-consistent manner the evolution of the viscosity of a thin disk and the formation of moonlets as well as the evolution of their orbits. The disk's surface density evolves under the action of both the viscous torque (proportional to the local viscosity, which itself depends on the local density at a distance r to the planet, see Daisaka et al., 2001) and the moons' gravitational torque exerted on the disk. The resulting governing equation is (Charnoz et al., 2010):

$$\frac{d\sigma}{dt} = \frac{3}{r}\frac{\partial}{\partial r}\left[r^{1/2}\frac{\partial(\nu(r)\sigma r^{1/2})}{\partial r} - \frac{1}{3\pi(GM_p)^{1/2}}r^{1/2}T(r)\right] \tag{2}$$

where σ and $\nu(r)$ are the surface density and the viscosity of the disk, respectively, G the universal constant of gravitation, and $T(r)$ is the sum over all the moonlets of the local Lindblad-resonance torque densities. This torque is induced by the mean motion resonances between the disk and the moonlets (see Charnoz et al., 2010).

In our model, the total mass of the disk is assumed to be initially 10^{18} kg accordingly to Craddock (2011), and the disk material is assumed to have a density of 3300 kg/m^3. The thermodynamical evolution of the disk (i.e. viscous heating, radiative cooling) is not taken into account, and the disk is assumed to be thin implying the disk's flattening is achieved. The initial surface density decreases as r^{-3}, and is set equal to zero at a distance of 90% of the Roche limit. The disk initially extends below the Roche limit in order to accurately study when it crosses the Roche limit since it is when moonlets form. The disk surface density reaches a maximal value of about 10^4 kg/m^2 (see Section 3.2.2), which is much closer to the density of the Saturn's A ring (about 400 kg/m^2) than the one of the protolunar disk (about 10^8 kg/m^2) close to the Earth. As the viscosity is proportional to σ^2/Ω_k^3 (where Ω_k is the Keplerian orbital frequency) for a marginally gravitationally unstable disk (Craddock, 2011), the viscosity of this circum-martian disk is of the same order of magnitude as the one of Saturn's A ring. So, the circum-martian disk would spread slowly as for Saturn's rings, thus creating many small moons (Charnoz et al., 2010) and the disk's viscous heating should be much less efficient than it is in the protolunar disk. The formation of moonlets is done via a simple algorithm: at each time-step of the numerical integration of Eq. (2), all disk material having crossed the Roche limit is removed from the hydrodynamical simulations (i.e. from Eq. (2)) and converted into a new moonlet. This algorithm was successfully used to account for the formation of Saturn's small moons (Charnoz et al., 2010, 2011).

Once formed, the moonlets are assumed to orbit Mars on near-circular orbits, which evolve due to gravitational interaction with both the planet (tidal decay due to Mars tides raised by the moonlets) and the disk (mean motion resonant interaction between the moonlets and the disk). Indeed, the gravitational torque exerted by the moonlets pushes disk material inward to the planet at the location of the resonances, and in order to balance the angular momentum of the system, a torque is exerted on the moonlet orbits, which pushes them outward from the planet. The evolution of the semi-major axis of the orbit of the moonlet is given by the following relationship (Charnoz et al., 2010):

$$\frac{da}{dt} = -\frac{3k_2 n_s m_s R_p^5}{Qa_s^4 M_p}\left[1 + \frac{51e_s^2}{4}\right] + \frac{2a_s^{1/2}\Gamma_s}{m_s(GM_p)^{1/2}} \tag{3}$$

with n_s, a_s, e_s, the mean motion, semi-major axis, and eccentricity of the moonlet orbit, respectively, m_s, its mass, M_p, R_p, k_2 and Q, the

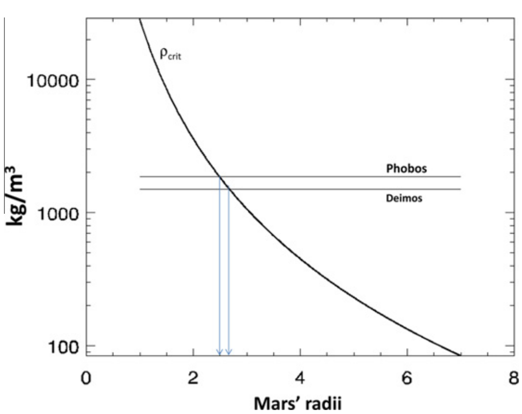

Fig. 1. Critical density of an object accreted in a gravitationally unstable circum-martian disk (strong tide regime) vs. the distance to the planet. Comparison with the density of Phobos and Deimos (see also Table 1).

Table 1
Shape (best-fit ellipsoid), mass and density of Phobos and Deimos from (1) Willner et al. (2010), (2) Thomas (1993), (3) Rosenblatt et al. (2008), (4) Jacobson (2010), (5) Rosenblatt (2011), (6) this study.

	Phobos	Deimos
Radius (in km)	13.0 × 11.39 × 9.07 (1)	7.5 × 6.185.2 (2)
Axes ratio	2.86:2.5:2 (6)	2.88:2.34:2 (6)
Mass (in 10^{16} kg)	1.06 (3)	0.151 (4)
density (in g/cm^3)	1.85 (5)	1.48 (5)

Table 2
Mars' physical constants taken into account in this study. (1) Konopliv et al. (2006), (2) Lainey et al. (2007), (3) Jacobson (2010).

Tidal potential Love number k_2	0.15 (1)
Tidal quality factor Q	80 (2,3)
Mass	6.42 10^{23} kg (1)

mass, radius, tidal potential Love number and tidal quality factor of Mars (see Table 2), respectively, and Γ_s the gravitational torque exerted by the disk on the moonlets. The contribution of the dissipation, due to tides raised by Mars inside the moonlets, to their orbital evolution is not taken into account since it is negligible with respect to the contribution of the dissipation inside the planet for near-circular orbits (e.g. Lambeck, 1979; Mignard, 1981). Moreover, eccentricity changes related to moonlet encounters are negligible, and do not have influence on the evolution of the system (Charnoz et al., 2010).

As the Roche limit (2.5 Mars' radii), where the moonlets formed, is well below the synchronous orbit (6 Mars' radii), the tidal interaction (first term of Eq. (3)) pushes the moonlets inward to the planet whereas the resonant interaction with the disk (second term of Eq. (3)) pushes the moonlet away from the planet. Therefore, two regimes of orbital evolution exist: outward and inward migration of the moonlets depending on the respective strength of the tidal and disk gravitational interaction. As the torque Γ_s is proportional to the disk's surface density and to the square of the moonlet mass (Charnoz et al., 2010), the ratio between the inward and the outward migration rates (i.e., the ratio between the first and second terms of Eq. (3)) is proportional to the disk's surface density (see Appendix A). Therefore, the transition from outward to inward migration regime is expected to take place when the disk's surface density drops below a threshold value (see Appendix A). This is a situation different from the case of Saturn where both tidal and disk gravitational interactions push the moonlets away from the planet because the outer edge of the rings, where gravitational instability takes place, is beyond the synchronous limit (Charnoz et al., 2010, 2011).

As in the case of Saturn's moons, the mutual accretion of moonlets is taken into account in the following way: when the semi-major axis of the orbit of two different moonlets differs by less than 2.5 times their Hill radii (given as $R_h = a(m_s/3M_p)^{1/3}$), they are considered as perfectly accreting, i.e. they assemble into one single larger body as in a low velocity two-body encounter (see Karjalainen, 2007).

On the basis of this model, we then study the evolution of both accreted moonlets and disk surface density, and we track the amount of disk material falling back to Mars.

3.2.2. Results

Due to its viscosity, the disk is radially spreading, and besides expanding begins to lose material through its inner edge. This material falls onto Mars, and its amount is about 5% of the disk initial mass after about 400 ka (Fig. 2), when the disk crosses the Roche limit and begins to lose additional material through its outer edge by forming moonlets (Fig. 3). Each moonlet has a mass ranging between about 10^{10} kg and 10^{13} kg, corresponding to Phobos-density bodies between 100 m and 1 km size, respectively. Within this population, individual moonlets continue to grow by accreting material from the outer edge of the disk or by mutual accretion, and can reach a mass of up to a few 10^{15} kg after about 14 Ma (Fig. 3), which is compatible with Deimos' mass but is lower than Phobos' mass (see Table 1).

Due to the gravitational interaction between the disk and the moonlets, the moonlets migrate away from the planet with a rate proportional to their mass (see Eq. (3)), resulting in a sorting among the moonlet population with the more massive moonlets at larger distances from Mars (Fig. 3), similarly to the case of Saturn's small moons (Charnoz et al., 2010, 2011). However, this orbital architecture is not the one of the current martian moon system, since the least massive moon, Deimos, orbits the farthest from the planet.

At about 70 Ma, the disk has lost almost 75% of its mass (Fig. 2), and its surface density has decreased by a factor of about 1/4 to 1/3 (Fig. 3). As a consequence, the viscosity (proportional to the square of the density, Charnoz et al., 2010) has also decreased, and the viscous torque can be overcome by the moonlet gravitational torque at the location of the strongest Lindbald resonances. When such a resonance is near the outer edge of the disk, the resulting moonlet gravitational torque stops the viscous spreading of the disk through the Roche limit, and eventually stops the production of moonlets (in our model after about 70 Ma, Fig. 3). The total mass of accreted moonlets is then 10^{16} kg, or 1% of the initial mass of the disk (Fig. 2), which corresponds to the mass of Phobos (see Table 1). However, at 70 Ma, the biggest moonlet has a mass still lower than Phobos' mass (Fig. 3).

The moonlet system continues its outward migration till about 100 Ma (Fig. 3). The disk has then lost about 90% of its initial mass (Fig. 2), and its surface density becomes too small to maintain a disk gravitational torque able to compensate for the tidal torque of the planet (see Appendix A). As a consequence, the moonlet orbits start to recede back to the planet (Fig. 3). As the more massive moonlets recede faster than the smaller ones, they accrete the less massive moonlets orbiting closer to Mars. As the mass of individual moonlets increase, their gravitational torques on the disk increase too, and stop outward spreading of disk's material at location of the lindblad resonances, and material accumulate just interior to these

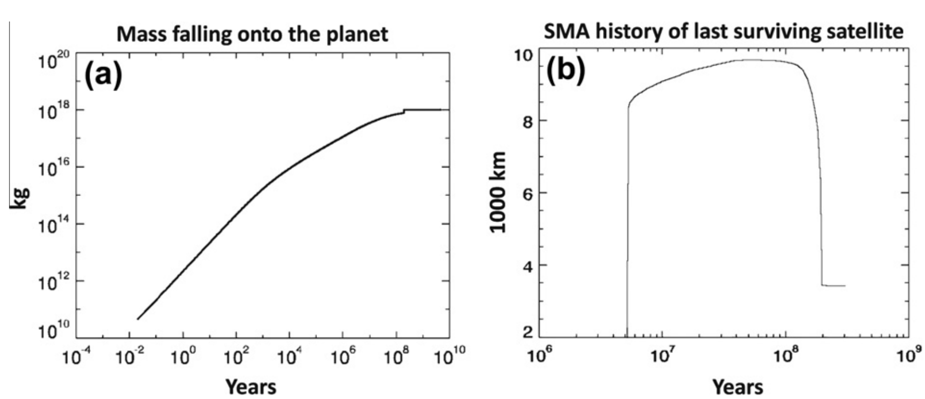

Fig. 2. History of (a) the disk's mass falling onto the planet and (b) the semi-major axis (SMA) of the orbit of the last surviving moonlet formed in the strong tide regime of accretion.

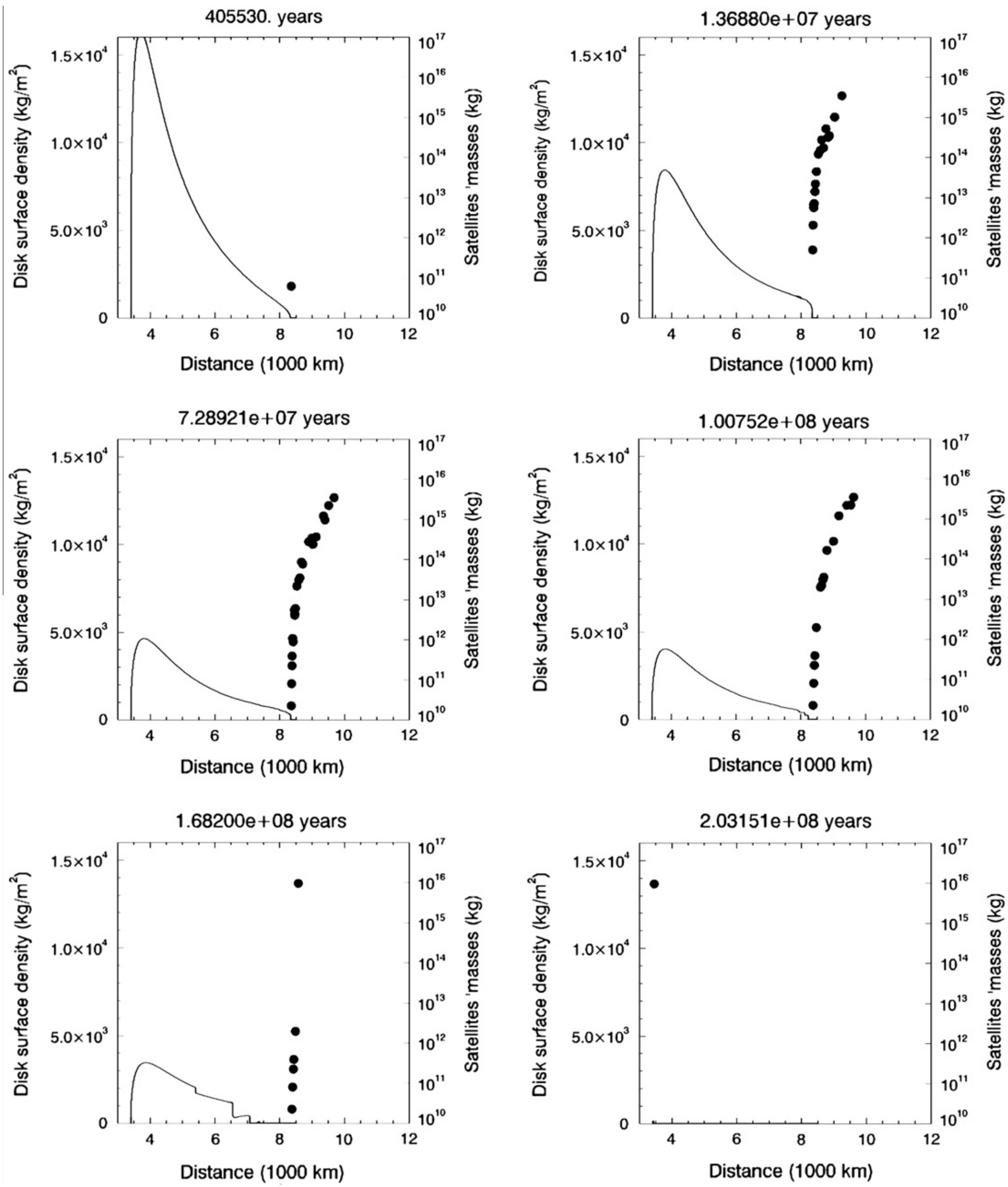

Fig. 3. Model of evolution of a gravitationally unstable circum-martian accretion disk (strong tide regime of accretion, see text for details).

resonances forming step-like features in the density profile (Fig. 3). Then, the entire disk is pushed inward to the planet by the inward migration of the moonlets, and the balance of the angular momentum of the system is now dominated by the moonlet-planet gravitational interaction. All the moonlets eventually accrete into one single massive object, which has thus accreted all the material previously extracted from the outer edge of the disk (i.e. 10^{16} kg, Fig. 3). This single massive object initiates the collapse of the disk onto Mars at about 200 Ma after the beginning of its evolution (Fig. 3), given the dissipation rate in Mars considered in our model (see Table 2).

The removal of whole the moonlet system in about 200 Ma is incompatible with the age estimate of the surfaces of the martian moons of at least 1 Ga (Pollack, 1977; Thomas and Veverka J., 1980). Moreover, in our model, the largest distance to Mars that the moonlets can reach is about 3 Mars' radii (or 10^4 km from Mars' center, Fig. 3). This distance results from the lowest order Lindblad resonances located at the outer edge of the disk, which can counterbalance the tidal torque of the planet. For a disk with a mass of 10^{18} kg, the 6:5 resonance can maintain a moonlet with a mass of a few 10^{15} kg at the 2.82 Mars' radii distance as long as the disk's surface density is above the threshold surface density (see Fig. 2, and Appendix A). Therefore, none of the moonlets formed at the Roche limit can reach the current location of Deimos beyond the synchronous orbit.

Our simulations have thus shown that the current martian moon system cannot result from accretion in a strong tide regime (i.e. at the Roche limit) in a disk of 10^{18} kg resulting from a giant impact having occurred early in Mars' history. Modifications of the model will be discussed in Section 5, especially the initial mass of the disk.

4. The weak tide regime of accretion

If the accretion of the martian moons occurred at distances larger than several times the Roche limit distance, then the effect of tides on the accretion process may have been very limited. In that case, accretion occurs in a somewhat classical accretion process in a disk, or in a somewhat similar way as for planet formation.

4.1. Basic physics

In this regime, we assume that the debris disk around Mars is gravitationally stable and can extend to the current orbit of Deimos. These assumptions could be reached if the disk has a relatively low density and/or is hot. Indeed, gravitational instabilities develop in a disk with relatively high viscosity (so, high density, see Salmon et al., 2010) and a hot disk can extend farther from the planet before cooling. If the disk is initially gaseous (because it is presumably very hot), one would expect at the beginning a strong pressure gradient (so that the disk is in thermal expansion after the impact). Therefore, a strong radial density gradient is very possible, for example when considering papers on protolunar disks formation (e.g. Canup, 2008). In this case the disk may expand rapidly through thermal expansion.

In addition, the disk may cool down on timescale much longer than the collisional timescale if the disk is initially hot and gaseous (for a pressure supported disk, the cooling mechanism is through black-body emission and not through collisional cooling). Indeed, in a recent paper by Ward (2012) about the protolunar disk, which is pressure supported, it is found that this protolunar disk cools down in about 40 years, which is about 1000 orbits because the disk photosphere is at a temperature of 2000 K. Whereas it is still unclear if a circum-martian disk may be wide and hot (rather than compact and cool), we consider both cases in the present papers.

In this regime material accumulation is similar to the accretion of planetary embryos from a disk of planetesimals as described in an abundant literature (e.g. Lissauer, 1987; Wetherill and Stewart, 1993 and references therein). For this kind of disk, a good approximation of the surface density $\sigma(r)$ is given as a power law function of the distance to the planet's center of mass as:

$$\sigma(r) = \sigma_0 r^q \tag{4}$$

with q between -0.5 and -5. In such a disk, accretion occurs via successive two-bodies low-velocity encounters (e.g. Greenberg et al., 1978; Lissauer, 1987; Spaute et al., 1991; Wetherill and Stewart, 1993 and references therein). In this regime of accretion, objects are formed with different sizes, and if the disk is cold enough (in terms of encounter velocities), a few big bodies can rapidly grow via the so-called runaway growth mechanism (e.g. Greenberg et al., 1978; Lissauer, 1987; Wetherill and Stewart, 1989; Spaute et al., 1991) since the larger a body becomes, the larger its gravitational cross section C_g will be (given as $C_g \approx \pi a^2 \left(1 + (V_{esc}/V_{rel})^2\right)$, with a and V_{esc}, the radius and the escape velocity of the body, respectively, and V_{rel} the relative or encounter velocity between the two accreting bodies). Due to the combination of dynamical friction and cooling from dissipative collisions, these encounter velocities are mostly comparable to the escape velocity of the bodies in which most of the mass is locally distributed (i.e. small bodies at the beginning of the disk evolution and bigger bodies at the end). As a result, the accretion by larger bodies is favored (since these bodies have escape velocities larger than relative velocities) and a finite number of bodies grow very rapidly, corresponding to runaway growth of big bodies, outlying from the size distribution of the system of accreted objects. These bodies are called "embryos". As the mass of the disk is progressively transferred into these embryos, the system progressively "heats-up" (Ida and Makino, 1993), and the relative velocity V_{rel} increases. Thus, this mechanism is a self-terminating process as embryos stir their environment and accrete all the material inside their gravitational reach. Lissauer (1987) has shown that there is a theoretical asymptotic mass, the isolation mass (M_i), which is reached when the embryo has cleaned up all the disk material in the neighborhood of its distance to the planet (i.e. inside a volume corresponding to a couple of its Hill sphere volume). The isolation mass depends on the mass of the planet, M_p, and on the amount of disk material available at the distance, r, to the planet according to (e.g. Lissauer, 1987):

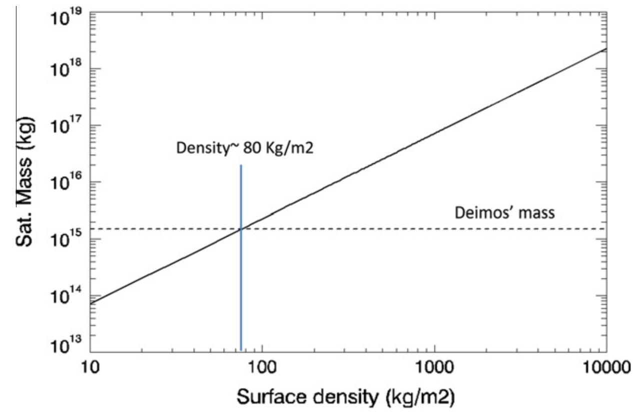

Fig. 4. Maximum growth mass (isolation mass) of an object (embryo) accreted in the weak tide regime near the current location of Deimos (6 Mars' radii) vs. the surface density of the accretion disk. Comparison with Deimos' mass (see Table 1).

$$M_i = \frac{\left(16\pi r^2 \sigma(r)\right)^{3/2}}{\left(3M_p\right)^{1/2}} \tag{5}$$

If one assumes that Deimos formed in such a regime of accretion, Eq. (5) shows that the surface density of the disk needed for an isolation mass matching the mass of Deimos must be about 80 kg/m^2 at 6 Mars' radii (Fig. 4), which corresponds to a total mass of the disk between 10^{17} kg and 10^{18} kg, depending on the q value of the disk's surface density profile (see Appendix B). This mass range just overlaps the lower threshold of the 10^{18}–10^{19} kg range estimated in Craddock (2011).

In order to accrete a Phobos in the same disk, the embryo has to be formed below the synchronous orbit in order to be compatible with the current location of Phobos around Mars, which requires $q < -2$ for the density profile of the disk and for distances to Mars of 3–4 Mars radii (Fig. B.1 in Appendix B). However, a Phobos-mass body at such close distances to Mars is expected to fall back onto Mars in less than 1 Ga due to the tidal decay of its orbit. In order to maintain such an embryo in Mars' orbit over 4.5 Gy, it is required to form it just below the synchronous orbit. In turn, a disk's surface density of about 290 kg/m^3 is needed, which is still compatible with a disk's mass of the order of 10^{18} kg. However, in such a denser disk, the embryos formed just beyond the synchronous orbit will have a mass larger than Deimos itself.

It is worthwhile to note that in the post-runaway growth stage (or oligarchic growth stage), slightly larger embryos are formed with an orbital separation of about 10 times their mutual Hill radii (Kokubo and Ida, 1998; Thommes et al., 2003). Although, the mass of these embryos is slightly larger than the isolation mass given in Eq. (5), it does not significantly change the results of this study (see Appendix B).

5. Discussion

In the strong tide accretion regime, several tens of moonlets can be formed from the viscous spreading of the accretion disk through the Roche limit. Although these moonlets have a shape and a density comparable to those of Phobos and Deimos, they cannot be maintained in Mars' orbit over billions of years. This is due to the fact that the disk is almost emptied in about 100 Ma, which then permits to remove whole the moonlets by tidal decay of their orbits in comparable timescales.

One may assume a denser (i.e. more massive) disk, which would dissipate more slowly and make the survival time of the moonlet system longer. For example, a disk 40 times more massive would have a survival time of 4 Ga (40 times 100 Ma), if one assumes the disk loses its material at the same rate as for an initial mass of 10^{18} kg. However, the mass fluxes, Φ, through the edges of a viscous spreading disk are larger for larger disk masses (e.g. $\Phi \propto M_{disc}^2$, see Salmon et al., 2010), and the disk could not be maintained over billions of years. In addition, a more massive disk would produce more massive moonlets (as the mass of the more massive moonlets increases with the initial mass of the disk, Charnoz et al., 2010, 2011), which will recede back to Mars faster since the rate of the tidal decay of their orbits is proportional to their mass. On the other hand, a less massive disk will evolve more slowly (Salmon et al., 2010), but will produce less massive moonlets, which could not reach the mass of Phobos.

In a denser (more massive) disk, lower order resonances could maintain moonlets at larger distances to Mars, but the maximal distance cannot be larger than the distance given by the 2:1 (lowest order) resonance located at the outer edge of the disk (corresponding to a distance of 4 Mars' radii for a disk outer edge located near the Roche limit at 2.5 Mars' radii). This is still below the synchronous orbit distance to Mars, thus the current location of Deimos cannot be reached by any moonlet formed in the strong tide regime of accretion whatever the initial mass of the disk. In order to try to account for the formation of Deimos in such a regime of accretion, we assume that the synchronous orbit was at closer distance to Mars at the time of formation of the moonlets. The synchronous limit should be at a distance of less than about 4 Mars' radii since this distance is the maximal distance that moonlets can reach when migrating outward from the planet (according to Craddock (2011), this may require a more massive impactor, which would have spun up Mars at a rate of about 13 h). In such a scenario, when the moonlets cross this closer-to-Mars synchronous orbit, both tidal interactions with Mars and the disk make their orbits migrating away from Mars (similarly to the Saturn's case, Charnoz et al., 2010, 2011), thus getting farther from Mars. However, since the most massive moonlets are at the largest distance from Mars (since the outward migration rate is proportional to the mass of the moonlet), and the disk must be massive because of the required massive impactor, the outer moonlets will have much larger masses than Deimos. In addition, a second collision with a suitable mass-impactor would be required in order to slow down Mars' spin rate from 13 h to its current value, since the tides raised by the Sun will not change Mars' rotation by about a factor of 2 in 4.5 Gy (Goldreich and Soter, 1966).

Although the strong tide regime of accretion cannot account for the current martian moon system, it does not mean that moonlets cannot have been formed in such a regime of accretion in Mars' early history. If Mars has had in the past a circumplanetary disk, our work simply implies that such an accretion process actually took place, and had produced one or more moonlets, which would have then crashed onto Mars, and fed the elongated crater population. To account for all of this population, the total mass of moonlets must be between 8.3×10^{17} kg and 1.5×10^{19} kg (see Section 3.1 in Craddock, 2011). Since our simulations show that only 1% of the disk material is used to produce moonlets, the disk must have had a mass between 8.3×10^{19} kg and 1.5×10^{21} kg (or about 0.86–15.6% of the mass of the Mars impactor). Although the lower bound of this range is about twice the upper bound of the 0.01–0.4% range estimated in Craddock (2011), it seems to be plausible given the large uncertainty in the mass ejected in orbit. Therefore, the total mass of moonlets, formed in a strong tide regime in a disk with a mass of about 10^{20} kg, can reach the total mass of impactors required to account for the elongated crater population. However, our study also shows that moonlets eventually accrete together when falling back onto Mars, thus it seems difficult to explain the 102–176 elongated craters observed at the martian surface from one or a few falling moonlets, unless the moonlets would have been broken into smaller pieces when crossing the Roche limit before impacting Mars. Such a fragmentation is not unplausible if the moonlet contains a significant amount of porosity in its interior (Movshovitz and Asphaug, 2011), which is particularly the case in our model if the disk material has a density of silicate rock (3300 kg/m^3).

In the weak tide regime, the embryos or moonlets, accreted between the Roche limit and the synchronous orbit, also offer a population of impactor-candidates for the elongated crater population at the martian surface. It is thus worthwhile to see whether the bulk characteristics of the expected embryo population is consistent with those of the elongated crater population. For a disk where a Deimos-mass body is accreted at the synchronous distance from Mars, the mass of the moonlets is between 10^{14} kg and 10^{17} kg depending on the q value of the disk's surface density profile (see Appendix B), which is well in agreement with the estimated range of the mass of the impactors having formed the elongated craters (see Appendices A and B in Craddock, 2011). Moreover, the more massive embryos are expected to orbit closer to Mars (for $q < -2$, see Fig. B.1 in Appendix B), and are therefore expected to fall back onto Mars before the less massive, more distant ones (since the orbital tidal decay rate is proportional to the moonlet mass). As a consequence, larger elongated craters would be formed first, which is consistent with the observations (i.e. the largest elongated craters are the oldest ones, Schultz and Lutz-Garihan, 1982; Buchenberger et al., 2011). However, the expected number of embryos formed in the disk is about 45–110 (depending on the q value considered for the surface density profile of the disk, see Fig. B.2 in Appendix B), which is less than the 102–176 elongated craters identified at the martian surface. This discrepancy between the number of moonlets and the number of elongated craters may be removed if one assumes that moonlets are broken in some pieces before impacting the surface. Alternatively, only a part of the elongated craters may result from decaying moonlets (Bottke et al., 2000; Herrick et al., 2012).

On the other hand, it may also be possible that neither Phobos nor Deimos are embryos but originate from merging of embryos. Indeed, numerous works on planetary formation have shown that the final stage of planetary growth is by mutual accretion of embryos. In the martian case, we can expect that embryos formed below and beyond the synchronous orbit may migrate inward to and outward from the planet, respectively, because of tidal effects, and form larger objects by mutual accretion. Moreover, it is likely to find enough embryos just below the synchronous orbit with a total mass corresponding to Phobos' mass. Indeed, in a disk with a mass of 10^{17}–10^{18} kg, the embryos near the synchronous orbit will have a mass close to the mass of Deimos, so that the accretion of only a few of them would permit reaching the mass of Phobos. However, it is not possible to conclude on the viability of such a scenario in the absence of detailed study with numerical simulations.

6. Conclusion

This study has investigated, for the first time, a physical basis for the formation of Phobos and Deimos from a circum-martian disk of accretion. In the light of current theories of accretion, two regimes of accretion have been explored: the strong tide and the weak tide regime.

In the strong tide regime, moonlets can be formed close to the planet by gravitational instabilities, when the viscous disk is spreading through the Roche limit (at about 2.5 Mars' radii). The shape and the density of Phobos and Deimos are consistent with those expected for these moonlets. For an initial mass of the disk of 10^{18} kg (Craddock, 2011), the total mass of all moonlets is 10^{16} kg, corresponding to the mass of Phobos. However, all martian moonlets orbit Mars below the synchronous orbit (lying at 6 Mars' radii), so that they recede back to Mars in less than 200 Ma. It is inconsistent with both the crater retention age of the surfaces of Phobos and Deimos, with the current position of Deimos around Mars, and with the scenario proposed in Craddock (2011). This evolution of the moonlet system is driven by the loss of disk material through its inner edge, which decreases its surface density. In turn, the strength of the gravitational torque exerted on the moonlet orbits by the disk decreases, and cannot permit to compensate for the tidal torque of the planet, making these orbits receding back to the planet. This is a different situation from the one of Saturn's small moons for which the Roche limit is beyond the synchronous orbit, which makes both disk and planet gravitational torques pushing moonlets away from the planet, and maintaining them in orbit for billions of years (Charnoz et al., 2010, 2011).

While the strong tide regime does not allow for the formation of martian moonlets beyond the synchronous orbit, the weak tide regime allows for the accretion of a Deimos-mass moonlet (as an embryo resulting from a runaway growth from smaller planetesimals) near the current distance of Deimos to Mars, given an initial mass of the accretion disk of up to 10^{18} kg. Within such a disk, a Phobos-mass moonlet can also be formed but at closer distance to Mars (3–4 Mars' radii), due to its larger mass than that of Deimos. However, at such distances to Mars, this accreted body is expected to fall back rapidly onto Mars due to the tidal decay of its orbit, and so not to survive over billions of years in Mars' orbit.

On another hand, in the weak tide regime, embryos can accrete together to form a reduced population of larger bodies. In that case, we only note that because of tidal effects, we may expect that embryos below the synchronous orbit may migrate inward and form larger objects, and embryos beyond the synchronous limit may migrate outward while growing bigger. Does such a process end in one single Phobos below the synchronous orbit and one single Deimos beyond the synchronous orbit? The present study does not answer that question, but it emphasizes that there is clearly a mechanism of accretion that must be investigated in the case of the formation of the martian moons.

Acknowledgments

The authors greatly thank two anonymous reviewers for their helpful comments, which have significantly clarified several points in the manuscript. P. Rosenblatt is financially supported by the Belgian PRODEX program managed by the European Space Agency in collaboration with the Belgian Federal Science Policy Office. P. Rosenblatt thanks A. Trinh for his help in solving for the number of embryos expected to be formed in a circum-martian accretion disk. T. van Hoolst is acknowledged for his thorough reading of a first version of the manuscript, which has allowed for some clarifications.

Appendix A. Strong tide regime: transition from outward to inward migration of moonlets

Hereafter, we analytically investigate the transition from the outward to the inward migration regime for the moonlet orbital evolution. This transition occurs when the tidal torque of the planet overcomes the disk gravitational torque exerted on the moonlets. This latter torque can be expressed as follows (Charnoz et al., 2010):

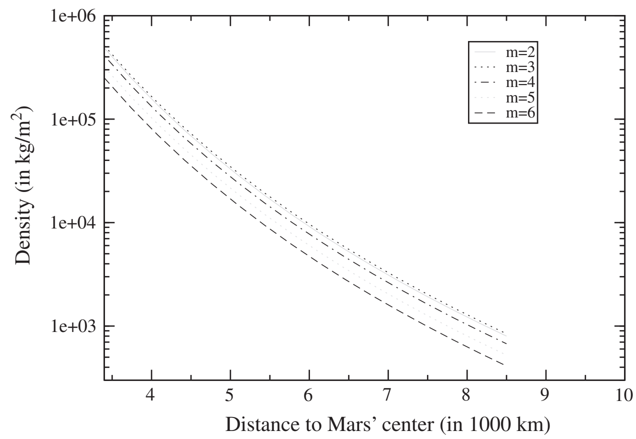

Fig. A.1. Strong tide regime: minimal (or threshold) surface density of the disk vs. the position in the disk and the order m of the Lindbald resonances. See text for details.

$$\Gamma_s = fm(m-1)\sigma(r)r^4\Omega^2\left(\frac{m_s}{M_p}\right)^2 \tag{A.1}$$

where f is a coefficient of about 10, m and r are the order and the distance to the planet of the Lindbald resonances within the disk, Ω is the orbital frequency at the distance r, m_s and M_p are the mass of the moonlet and of the planet, respectively, and $\sigma(r)$ is the disk surface density at the distance r. Whereas not perfect, this approximation gives a good first order idea of the system evolution. Indeed, as the outward migration rate is proportional to Γ_s (see Eq. (3)), it becomes lower than the inward migration rate when the absolute value of the first term of Eq. (3) is larger than the one of the second term, i.e. when the following condition on the disk surface density is achieved:

$$\sigma(r) \leqslant \frac{3k_2M_pR_p^5(m-1)^3}{2Qfm^5r^7} \tag{A.2}$$

where k_2, Q and R_p are the tidal Love number, the tidal quality factor and the radius of the planet, respectively (see Table 2). The second term of Eq. (A.2) can be seen as the minimal or threshold disk surface density corresponding to the transition between the outward and the inward migration regimes. The timescale of the moonlet system evolution is thus driven by this threshold density, which only depend on the planet characteristics and on the order and the position of the Lindbald resonances resulting from the gravitational interaction between the disk and the moonlets. This minimal density is the lowest at the outer edge of the disk and for increasing order of the resonances (Fig. A.1). In our simulations, with an initial mass of 10^{18} kg, the minimal density is as low as about 630 kg/m^2 for $m = 6$ at a distance of 8000 km, which corresponds to the lowest order resonance induced by the farthest moonlet located at about 2.82 Mars' radii (Fig. 3). The disk's surface density drops below this minimal density at about 100 Ma after the beginning of the disk evolution, when the farthest moonlet starts to recede back to Mars (Fig. 3).

Appendix B. Weak tide regime: analytical insight into number and mass distribution of embryos within the accretion disk

When matching the isolation mass to Deimos' mass, a disk's surface density of about 80 kg/m^2 is required near the synchronous orbit (6 Mars' radii from Mars' center, Fig. 4). Thus, one can compute the constant term in Eq. (4) as $\sigma_0 = 80/(6R_p)^q$ in order to derive disk's surface density profiles for different values of the

Table 3
Weak tide regime: total mass of the disk required to get embryo's mass (isolation mass) matching Deimos' mass at 6 Mars' radii of distance to Mars, for different disk's surface density profiles, as given by the value of the q exponent (see Eq. (4)).

q exponent value	Disk's mass (in kg)
−0.5	1.02×10^{17}
−1	1.22×10^{17}
−2	1.83×10^{17}
−3	2.93×10^{17}
−4	4.98×10^{17}
−5	8.94×10^{17}

exponent q. The total mass of the disk can then be computed by integrating those profiles over the disk extending from 2.5 Mars' radii (Roche limit) to 6 Mars' radii (synchronous orbit). The results are given in Table 3, and are not significantly modified if the outer limit of the disk is extended well beyond the synchronous orbit.

These profiles can also be used for computing the isolation mass vs. the distance to Mars for different values of q (Fig. B.1). For $q < -2$, the isolation mass decreases as the distance to Mars increases. As Phobos' mass is about 7 times larger than Deimos' mass, this implies that an embryo with Phobos' mass should be formed at 3 and 4 Mars' radii for $q = -4$ and $q = -5$, respectively (Fig. B.1).

The isolation mass is reached when the embryo has cleaned up all the disk material in the neighborhood of its distance to the planet (about 10 times its Hill sphere radius around its orbit, Kokubo and Ida, 1998, 2000; Thommes et al., 2003). Under this assumption, one can compute the number of embryos formed in a circum-martian accretion disk extending from 2.5 Mars' radii to 6 Mars' radii as follows:

$$a_{i+1} = a_i + 10\left(\frac{M_{i+1} + M_i}{3M_p}\right)^{1/3}\left(\frac{M_{i+1}a_{i+1} + M_i a_i}{M_{i+1} + M_i}\right) \tag{A.3}$$

where M_{i+1} and M_i are the isolation masses at the a_{i+1} and a_i distances to Mars, respectively, M_p is the mass of the planet, and the index i corresponds to the ith embryo from the Roche limit. The total number N of embryos is thus obtained when the distance a_N reaches the synchronous orbit. This number depends on the surface density profile of the disk, and is ranging from about 45 for $q = -5$ to about 110 for $q = -0.5$ (Fig. B.2).

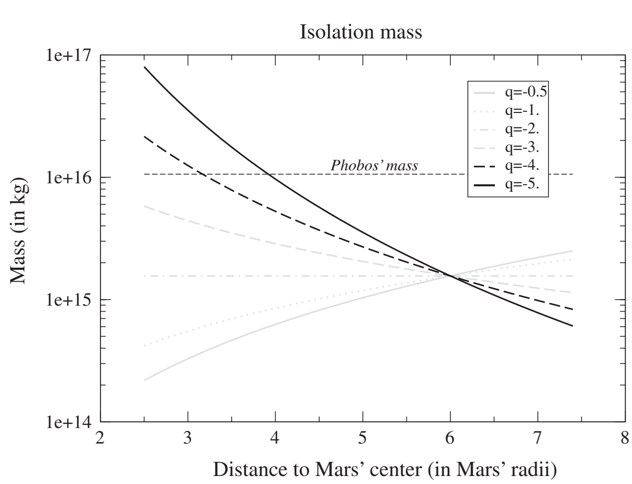

Fig. B.1. Weak tide regime: isolation mass vs. the distance to Mars' center for different values of the q exponent of the disk's surface density profile (see Eq. (4)). Each isolation mass profile matches Deimos' mass at 6 Mars' radii to Mars.

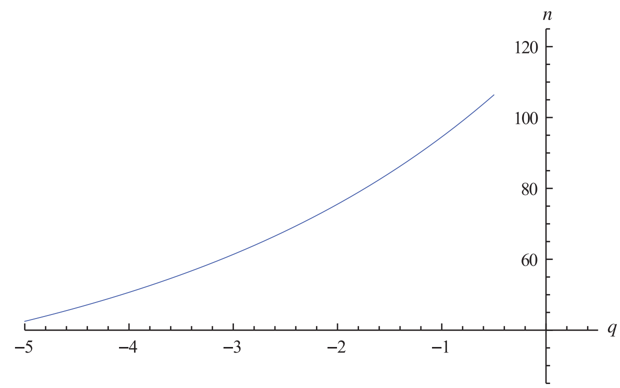

Fig. B.2. Weak tide regime: expected number of embryos accreted in a circum-martian disk extending from the Roche limit (2.5 Mars' radii) to the synchronous orbit (6 Mars' radii) for different values of the q exponent of the disk's surface density profile (see Eq. (4)).

In the oligarchic growth mode, the embryos are slightly larger than in the runaway growth mode. Their mass M is given as (according to Kokubo and Ida, 2000):

$$M = 2\pi abp\sigma(a) \tag{A.4}$$

where $\sigma(a)$ is the surface density of the solid material in the disk at the orbital distance a to Mars, p the ratio of the total mass of embryos to the mass of the disk, and b is the orbital separation between embryos. The final mass of the embryos, M_f, is obtained for $p = 1$ and $b = 10R_h$, with $R_h = a(M/3M_p)^{1/3}$ (according to Kokubo et al., 2000) as follows:

$$M_f = \frac{(20\pi a^2\sigma(a))^{3/2}}{(3M_p)^{1/2}} \tag{A.5}$$

This mass is only 40% larger than the isolation mass given by Lissauer (1987). When applying this new mass of embryo to our estimate of the circum-martian disk surface density at 6 Mars' radii, as obtained to match Deimos' mass, it yields to a value of 64 kg/m^2, which is in the same order of magnitude as the 80 kg/m^2 value obtained using the Lissauer (1987) isolation mass (see Section 4). The total mass of the disk associated with the disk surface density of 64 kg/m^2 is only 25% lower than the total mass estimated in Table 3. In addition, the number of embryos estimated by using this new embryo mass is between 40 and 100, which is not significantly different from the 45 to 110 range obtained by using the isolation mass of Lissauer (1987).

References

Andert, T.P., Rosenblatt, P., Pätzold, M., Häusler, B., Dehant, V., Tyler, G.L., et al., 2010. Precise mass determination and the nature of Phobos. Geophys. Res. Lett. 37. http://dx.doi.org/10.1029/2009GL041829.
Bottke, W.F., Love, S.G., Tytell, D., Glotch, T., 2000. Interpreting the elliptical crater population on Mars, Venus, and the Moon. Icarus 145, 108–121.
Brahic, A., Henon, M., 1977. Systems of colliding bodies in a gravitational field. II – Effect of transversal viscosity. Astron. Astrophys. 59 (1), 1–7.
Buchenberger, B., Witasse, O., Loizeau, D., Chicarro, A., Rosenblatt, P., 2011. Elongated craters on Mars revisited: Test of the decaying moonlets hypothesis? EPSC-DPS2011, Nantes, France, 2–7 October 2011. Abstract 738.
Burns, J.A., 1992. Contradictory clues as to the origin of the martian moons. In: Kieffer, H.H., Jakosky, B.M., Snyder, C.W., Matthews, M.S. (Eds.), Mars. Univ. of Ariz. Press, Tucson, Ariz, pp. 1283–1301.
Cameron, A.G.W., 1986. The impact theory for origin of the Moon. In: Hartmann, W.K., Phillips, R.J., Taylor, G.J. (Eds.), Origin of the Moon. Lunar and Planetary Institute, Houston, pp. 609–616.
Canup, R.M., 2004. Simulations of a late lunar-forming impact. Icarus 168, 433–456.
Canup, R.M., 2008. Lunar-forming collisions with pre-impact rotation. Icarus 196, 518–538.
Canup, R.M., Esposito, L.W., 1997. Evolution of the G ring and the population of macroscopic ring particles. Icarus 126 (1), 28–41.
Charnoz, S., Salmon, J., Crida, A., 2010. The recent formation of Saturn's moonlets from viscous spreading of the main rings. Nature 465, 752–754.

Charnoz, S., Crida, A., Castillo-Rogez, J.C., Lainey, V., Dones, L., Karatekin, Ö., Tobie, G., Mathis, S., Le Poncin-Lafitte, C., Salmon, J., 2011. Accretion of Saturn's mid-sized moons during the viscous spreading of young massive rings: Solving the paradox of silicate-poor rings versus silicate-rich moons. Icarus 216, 535–550.
Craddock, R.A., 2011. Are Phobos and Deimos the result of a giant impact? Icarus 211, 1150–1161.
Daisaka, H., Tanaka, H., Ida, S., 2001. Viscosity in dense planetary rings with self-gravitating particles. Icarus 154, 296–312.
Giuranna, M. et al., 2011. Compositional interpretation of PFS/MEX and TES/MGS thermal infrared spectra of phobos. Planet. Space Sci.. http://dx.doi.org/10.1016/j.pss.2011.01.019.
Goldreich, P., Soter, S., 1966. Q in the Solar System. Icarus 5, 375–389.
Greenberg, R., Hartmann, W.K., Chapman, C.R., Wacker, J.F., 1978. Planetesimals to planets – Numerical simulation of collisional evolution. Icarus 35, 1–26.
Herrick, R.R., Schenk, P.M., Robbins, S.J., 2012. Surveys of elliptical crater population on the saturnian satellites, Mercury, and Mars. Icarus. http://dx.doi.org/10.1016/j.icarus.2012.05.027.
Ida, S., Makino, J., 1993. Scattering of planetesimals by a protoplanet – Slowing down of runaway growth. Icarus 106, 210–227.
Jacobson, R.A., 2010. The orbits and masses of the martian satellites and the libration of Phobos. Astron. J. 139, 668–679.
Karjalainen, R., 2007. Aggregate impacts in Saturn's rings. Icarus 189, 523–537.
Karjalainen, R., Salo, H., 2004. Gravitational accretion of particles in Saturn's rings. Icarus 172, 328–348.
Kokubo, E., Ida, S., 1998. Oligarchic growth of protoplanets. Icarus 131, 171–178.
Kokubo, E., Ida, S., 2000. Formation of protoplanets from planetesimals in the Solar nebula. Icarus 143, 15–27.
Kokubo, E., Ida, S., Makino, J., 2000. Evolution of a circumterrestrial disk and formation of a single Moon. Icarus 148, 419–436.
Konopliv, A.S., Yoder, C.F., Standish, E.M., Yuan, D.N., Sjogren, W.L., 2006. A global solution for the Mars static and seasonal gravity, Mars orientation, Phobos, and Deimos masses, and Mars ephemeris. Icarus 182, 23–50.
Lainey, V., Dehant, V., Pätzold, M., 2007. First numerical ephemerides of the martian moons. Astron. Astrophys., 465. http://dx.doi.org/10.1051/0004-6361:20065466.
Lambeck, K., 1979. On the orbital evolution of the martian satellites. J. Geophys. Res. 84 (B10), 5651–5658.
Lissauer, J.J., 1987. Timescales for planetary accretion and the structure of the protoplanetary disk. Icarus 69, 249–265.
Mignard, F., 1981. Evolution of the martian satellites. Mon. Not. R. Astr. Soc. 194, 365–379.
Movshovitz, M., Asphaug, E., 2011. Long term stability of a rubble-pile Phobos. EPSC-DPS2011, Nantes, France, October 3–7, 2011. Abstract 1654.
Peale, S.J., 2007. The origin of the natural satellites. In: Schubert, G., Spohn, T. (Eds.), Treatise on Geophysics, vol. 10, pp. 465–508.
Pollack, J.B., 1977. Phobos and Deimos: A review. In: Burns, J.A. (Ed.), Planetary Satellites. Univ. of Ariz. press, Tucson, Ariz, pp. 319–345.
Porco, C.C., Thomas, P.C., Weiss, J.W., Richardson, D.C., 2007. Saturn's small inner satellites: Clues to their origins. Science 318 (5856), 1602.
Rosenblatt, P. et al., 2008. Accurate Mars Express orbits to improve the determination of the mass and ephemeris of the martian moons. Planet. Space Sci. 56. http://dx.doi.org/10.1016/j.pss.2008.02.004.
Rosenblatt, P., 2011. The origin of the martian moons revisited. Astron. Astrophys. Rev. 19 (1), 19–44.
Safronov, V.S. et al., 1986. Protosatellite swarms. In: Burns, J.A., Matthews, M.S. (Eds.), Satellites. Univ. of Ariz. Press, Tucson, Ariz, pp. 89–116.
Salmon, J., Charnoz, S., Crida, A., Brahic, A., 2010. Long-term and large-scale viscous evolution of dense planetary rings. Icarus 209, 771–785.
Schultz, P.H., Lutz-Garihan, A.B., 1982. Grazing impacts on Mars: A record of lost satellites. J. Geophys. Res. 13 (Suppl. 87), A84–A96 (Proc. Lunar Sci. Conf.).
Singer, S.F., 2007. Origin of the martian satellites Phobos and Deimos. In: First International Workshop on the Exploration of Phobos and Deimos, Moffett Field, CA, USA, November 5–7, 2007. Abstract 7020.
Spaute, D., Weidenschilling, S.J., Davis, D.R., Marzari, F., 1991. Accretional evolution of a planetesimal swarm. I – A new simulation. Icarus 92, 147–164.
Thomas, P.C., 1993. Gravity tides and topography of small satellites and asteroids application to surface features of the martian satellites. Icarus 105, 326–344.
Thomas, P., Veverka, J., 1980. Crater densities on the satellites of Mars. Icarus 41, 365–380.
Thommes, E.W., Duncan, M.J., Levison, H.F., 2003. Oligarchic growth of giant planets. Icarus 161, 431–455.
Ward, W.R., 2012. On the vertical structure of the protolunar disk. Astrophys. J. 744, 140 (11 p.).
Wetherill, G.W., Stewart, G.R., 1989. Accumulation of a swarm of small planetesimals. Icarus 77, 330–357.
Wetherill, G.W., Stewart, G.R., 1993. Formation of planetary embryos – Effects of fragmentation low relative velocity and independent variation of eccentricity and inclination. Icarus 106, 190–209.
Willner, K. et al., 2010. Phobos control points network, rotation, and shape. Earth Planet. Sci. Lett. 294, 541–546.